

# Multi-Modal Deep Clustering: Unsupervised Partitioning of Images

Guy Shiran

The Hebrew University of Jerusalem

guy.shiran@mail.huji.ac.il

Daphna Weinshall

The Hebrew University of Jerusalem

daphna@cs.huji.ac.il

## Abstract

The clustering of unlabeled raw images is a daunting task, which has recently been approached with some success by deep learning methods. Here we propose an unsupervised clustering framework, which learns a deep neural network in an end-to-end fashion, providing direct cluster assignments of images without additional processing. Multi-Modal Deep Clustering (MMDC), trains a deep network to align its image embeddings with target points sampled from a Gaussian Mixture Model distribution. The cluster assignments are then determined by mixture component association of image embeddings. Simultaneously, the same deep network is trained to solve an additional self-supervised task. This pushes the network to learn more meaningful image representations and stabilizes the training. Experimental results show that MMDC achieves or exceeds state-of-the-art performance on five challenging benchmarks. On natural image datasets we improve on previous results with significant margins of up to 11% absolute accuracy points, yielding an accuracy of 70% on CIFAR-10, 31% on CIFAR-100 and 61% on STL-10.

## 1. Introduction

Clustering involves the organization of data in an unsupervised manner, based on the distribution of datapoints and the distances between them. Since these properties are closely tied to the representation of the data, the problems of clustering and data representation are firmly connected and are therefore sometimes solved jointly. In accordance, in this work we start from a recent method for the unsupervised computation of effective data representation (or features discovery), and develop a clustering method whose results significantly improve the state of the art in the clustering of natural images. The method is illustrated in Fig 1.

A large body of work has been devoted to the problem of clustering [21], see Section 2 for a brief review of some recent related work. The task of unsupervised image clustering is challenging and interesting, as the algorithm needs to discover patterns in highly entangled data, and produce

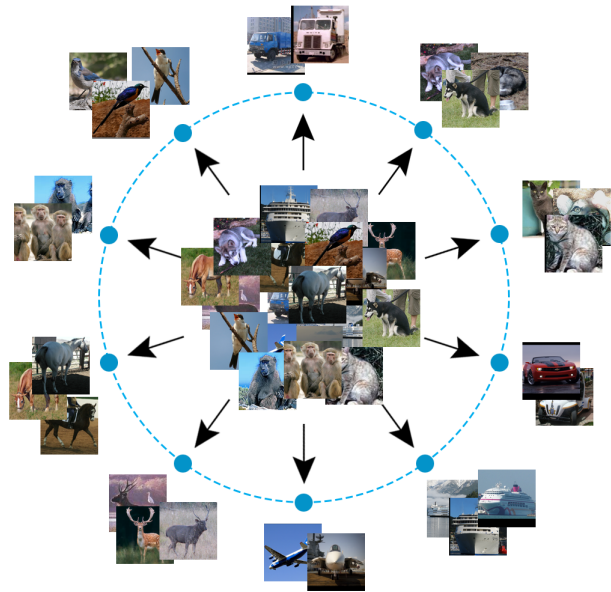


Figure 1. Our algorithm partitions a set of images into  $k$  clusters by aligning image embeddings of a deep network with target points sampled from a Gaussian Mixture Model on the  $k$ -dimensional unit sphere.

separated groups without explicitly specifying the grouping features. In recent years, with the emergence of deep learning as the method of choice in visual object recognition and image classification, emphasis has shifted to the computation of effective representations that will support successful clustering [31]. Vice versa, unsupervised clustering loss has been used to drive the computation of image representation and the discovery of enhanced image features by making it possible to use unsupervised data in the training of deep networks, which traditionally require massive amounts of labeled data.

When learning feature representation from unsupervised data by minimizing a clustering-based loss function, one danger is cluster collapse - the representation may collapse to the trivial solution of a single cluster. In [3], a similar

problem of representation collapse is managed by mapping the network’s representation to a fixed set of randomly chosen points in some target features space. Here we borrow this mapping idea, and incorporate it into a clustering algorithm.

More specifically, we first sample a fixed set of points in some target space. Since our method is designed to partition the data into  $k$  clusters, the target points are chosen from a matched density function - Gaussian Mixture Model (GMM) with  $k$  components. Our model trains a randomly initialized neural network to align its image embeddings with the sampled target points, directly inducing a partition that is based on the mixture components. This is done by simultaneously learning a one-to-one mapping between the output of the network and the target points, and updating the networks parameters to best fit images with their target points as assigned by the mapping.

In the absence of ground truth, the proposed approach is prone to instability as target points are continuously reassigned between images, creating a non-stationary online learning environment. Such instability is often linked with unsupervised learning tasks. To alleviate this problem, unsupervised tasks such as representation learning may be combined with self-supervision tasks to achieve better results [10]. Here we adopt the approach taken by [7] to deal with the notorious instability of training generative adversarial networks. Thus the model is jointly trained on the main clustering task and on a self-supervised auxiliary task as defined in RotNet [15], where all images are subjected to 4 rotation angles. In this auxiliary task the network is trained to recognize the 2D rotation of the image.

As its computation engine, our method uses off the shelf convnets and standard SGD training with mini-batch sampling in an end-to-end fashion. It is therefore scalable to large datasets. We evaluate our method on several standard benchmarks in image clustering and achieve or exceed state of the art results. In all the reported experiments, the same set of hyper-parameters is used.

The rest of the paper is organized as follows: In Section 2 we briefly review recent related work. In Section 3 we describe our method in detail and elaborate on its various ingredients. Experimental results are reported in Section 4.

## 2. Related work

**Data clustering.** The objective of data clustering is to partition data points into groups such that points in each group are more similar to each other than to data points in the other groups. Traditionally, clustering methods have been divided into density-based methods [24], partition-based methods [12], and hierarchical methods [11]. Partition-based methods, such as the popular k-means [33, 1], minimize a given clustering criterion by iteratively relocating data points between clusters until a (locally) optimal partition is attained.

Density-based methods define clusters as areas with high density of points, separated by areas with low density of points [38]. Hierarchical based methods build a hierarchy of clusters in a top-to-bottom [35] or bottom-to-top [17] manner to determine clustering.

**Representation Learning.** Naïvely attempting to cluster images with traditional approaches does not produce pleasing partitions of the images, as they work on the raw representations of the images in pixel space, and semantically similar images are not necessarily similar in the high-dimensional pixel space the images reside in. In recent years learning useful image representations in an unsupervised manner has been dominated by deep-learning-based approaches. Autoencoders (AEs) [2] encode images with a deep network and are trained by reconstructing the image using a decoder network. These include several variations such as sparse AEs, denoising AEs [37], and more [29, 43]. Generative models such as Generative Adversarial Networks (GAN) [16] and variational autoencoders (VAE) [23] learn representations as a byproduct of learning to generate images. Tightly connected to our work, Noise-As-Targets (NAT) [3] and DeepCluster [4] adopt a training strategy of iteratively reassigning pseudo-labels to points while training the network to fit them (see Section 3).

**Self-supervised learning.** A family of unsupervised learning algorithms that gained popularity in recent years are self-supervised methods. They learn representations by training a deep network to solve a pretext task, where labels can be produced directly from the data. Such tasks can be jigsaw puzzle solving [32], predicting the relative position of patches in an image [9], generating image regions conditioned on their surroundings [34], or more recently predicting image rotations (RotNet) [15]. In self-supervised GANs [7], predicting image rotations is used as an auxiliary task to stabilize and improve training, by enhancing the discriminators representation capabilities. This is an approach we adopt as well and elaborate on later on.

**Deep clustering.** The dominant and most successful approach to clustering of images in recent years has been to incorporate the tasks of representation learning and clustering into a single framework. Prominent works in the past years have been Joint Unsupervised Learning (JULE) [41], where the authors adopt an agglomerative clustering approach by iteratively merging clusters of deep representations and updating the networks parameters. Deep Adaptive Clustering (DAC) [5] recasts the clustering problem into a binary pairwise-classification framework, where cosine distances between image features of image pairs are used as a similarity measure to decide if they belong to the same cluster. Associative Deep Clustering (ADC) [18] jointly

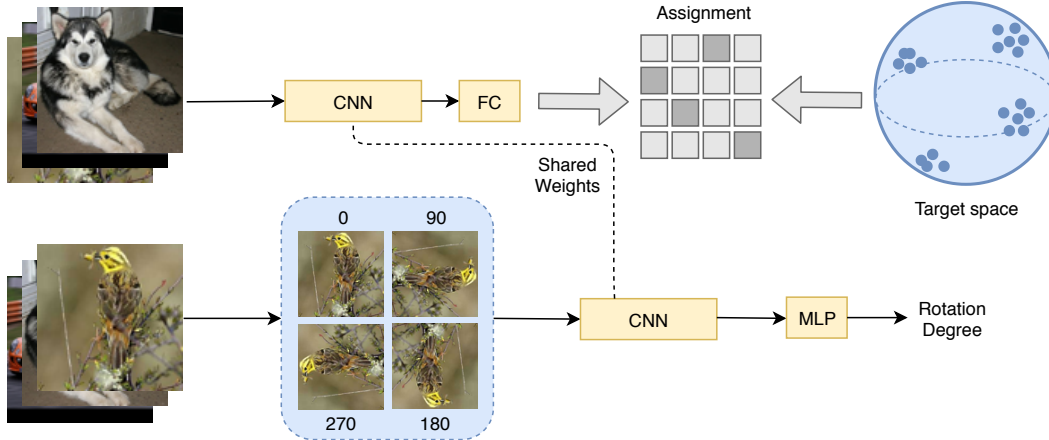


Figure 2. Our approach takes a set of images and solves two tasks in alternating epochs. In the primary task, a CNN is trained to produce output which matches some predefined set of target points sampled from a Gaussian mixture model, and optimally aligned with the training set. In the secondary task, given a rotated image, the same CNN is trained to predict the rotation angle of the image.

learns network parameters and embedding centroids with an association loss in order to estimate cluster membership. More recently, Invariant Information Clustering (IIC) [22] adopts an approach that achieves clustering based on maximizing the mutual information between two sets: deep embeddings of images, and instances of the images that underwent random image transformations while keeping the image semantic meaning intact. IIC leverages auxiliary over-clustering to increase expressivity in the learned feature representation, improving the representation capabilities of its network. This tactic bears resemblance to our incorporation of rotation prediction as an auxiliary task.

### 3. Method

Our task is to partition a set of images into  $k$  clusters, which reflect internal structure in the data. Fig. 2 shows an overview of the proposed approach. The algorithm alternates between solving the main unsupervised clustering task, and an auxiliary self-supervised task that helps the training process. The ingredients of the method are described next. The full method is summarized in Algorithm 1.

#### 3.1. Unsupervised learning

The starting point for this work is an unsupervised learning framework for learning image representation from unlabeled data. The method, Noise as Targets (NAT, Bojanowski & Joulin [3]), learns useful representations of images by training a deep network to align its images' embeddings with a fixed set of target points. The target points are uniformly scattered on the  $d$ -dimensional unit sphere.

More specifically, let  $X = \{x_i\}_{i=1}^n$  denote a set of images, and  $f_\theta : X \rightarrow Z$  the parameterized deep network

we wish to train. The output of  $f_\theta$  is normalized to have  $\ell_2$  norm of 1, entailing that  $Z$  is the  $d$ -dimensional unit sphere. NAT starts by uniformly sampling  $n$  targets on this unit sphere. Let  $\{t_i\}_{i=1}^n$  denote the set of target points, which remain fixed throughout the training. Each image  $x_i$  is assigned a unique target  $y_i$  through a permutation  $P : [n] \rightarrow [n]$ . The optimization objective is formulated as

$$\min_{\theta, P} \frac{1}{n} \sum_i \ell(f_\theta(x_i), y_i) \quad y_i = t_{P(i)} \quad (1)$$

where  $\ell$  is the Euclidean distance.

This optimization problem is solved in a stochastic manner, by iteratively solving it for mini-batches. Given a mini-batch of images  $X_b$ , the current representation vectors  $f_\theta(X_b)$  are first computed. Subsequently, Equation (1) is optimized for  $P$  over the points in mini-batch  $X_b$  using the Hungarian method [26], which reassigns the currently assigned targets of the mini-batch to minimize the Euclidean distance ( $\ell_2$ ) between images and their assigned target points. Finally, the gradients of  $f_\theta$  on  $X_b$  with respect to  $\theta$  are computed, and an SGD step is executed.

Intuitively, NAT permutes the assignment of image representation vectors to target points delivered by  $f_\theta$ , so that nearby embedding vectors are mapped to nearby target vectors, and then updates  $\theta$  accordingly. This process leads to the grouping of semantically similar images in target space, and to effective representations that perform well in downstream computer vision classification and detection tasks.

#### 3.2. Multi-modal distribution of target points

The uniform distribution of target points on the unit sphere, as described above, is not well suited for unsupervised clustering, since it is likely to blur the dividing lines

---

**Algorithm 1:**

---

**input:**  $\{x_i\}_{i=1}^n$  - images  
 $f_\theta$  - convnet with two heads  
 $k$  - number of clusters  
 $epochs$  - number of epochs to train  
 $iters$  - number of iterations in an epoch  
 $\sigma$  - variance of normal distribution  
 $d$  - dimension of embedding space  
 $\lambda_c, \lambda_r$  - learning rates  
 $g$  - random image transformation  
 $r$  - number of instances of  $g$  in a batch

$P \leftarrow$  initialize with random assignments  
 $\theta \leftarrow$  initialize with random weights  
 $T \leftarrow$  initialize empty list

**for**  $i = 1 \dots n$  **do**  
  sample  $c \sim \text{Categ}(\frac{1}{K}, \dots, \frac{1}{K})$   
  sample  $u \sim N(\mu_c, \sigma \cdot I_{d \times d})$   
   $T[i] \leftarrow t_i = \frac{u}{\|u\|}$   
**end**

**for**  $e = 1 \dots epochs$  **do**  
  **for**  $i = 1 \dots iters$  **do**  
    sample batch  $X_b$  and assigned targets  $T_b$   
    compute  $f_\theta(X_b)$   
    update  $P$  by minimizing Equation (1) w.r.t  $P$   
     $\bar{X}_b \leftarrow$  initialize empty list  
    **for**  $i = 1 \dots r$  **do**  
       $\bar{X}_b.append(g(X_b))$   
    **end**  
    compute  $\nabla_\theta L_c(\theta)$  of Equation (1) for  $\bar{X}_b$   
    update  $\theta \leftarrow \theta - \lambda_c \nabla_\theta L_c(\theta)$   
  **end**  
  **for**  $i = 1 \dots iters$  **do**  
    sample batch  $X_b$   
    rotate  $X_b \forall r \in \{0^\circ, 90^\circ, 180^\circ, 270^\circ\}$   
    compute  $\nabla_\theta L_r(\theta) // L_r$  is cross-entropy loss  
    update  $\theta \leftarrow \theta - \lambda_r \nabla_\theta L_r(\theta)$   
  **end**  
**end**

---

between clusters rather than sharpen them. Instead, multi-modal distribution seems like a natural choice for the objective of clustering, as it directly produces separated groups in target space.

In this work, we propose to use the mixture of Gaussians distribution, projected to the unit sphere, for the sampling of target points. Formally, this implies:

$$p(u) = \sum_{k=1}^K \alpha_k \cdot p_k(u) \quad u \in \mathbb{R}^d \quad (2)$$
$$p(t_i) = \int_{\frac{u}{\|u\|_2} = t_i} p(u) du \quad t_i \in Z$$

where  $K$  denotes the number of Gaussians in the mixture,  $d$  the dimension of the embedding space,  $\alpha_{k=1..K}$  a categorical random variable, and  $p_k(u)$  the multivariate normal distribution  $N(\mu_k, \Sigma_k)$ , parameterized by mean vector  $\mu_k$  and covariance matrix  $\Sigma_k$ . In the absence of prior knowledge we assume that the mixture components are equally likely, namely  $\alpha_k = \frac{1}{K} \forall k \in [K]$ . Finally, since the target points are constrained to lie on the unit sphere, we project the sample in  $\mathbb{R}^d$  to the unit sphere by  $t_i = \frac{u}{\|u\|_2}$ .

We define the cluster assignment  $c_i$  of image  $x_i$  as follows

$$c_i = \arg \min_k \|f_\theta(x_i) - \mu_k\|_2 \quad (3)$$

Note that if the final network  $f_\theta$  fits that target points exactly, namely  $f_\theta(x_i) = y_i$ , and if  $\Sigma_k$  are the same  $\forall k$ , then with high probability  $c_i$  is the index of the mixture component from which target point  $y_i$  has been sampled.

### 3.3. Random image transformations

Data augmentation is a useful and common technique to improve performance of machine learning algorithms. Usually, random image transformations such as cropping, flipping, rotation, scaling and photometric transformations are applied to images in order to expand the dataset with new and unique images. In our task of unsupervised clustering, these random transformations are essential, because they provide several instances of the same image that appear different but share the same semantic meaning as they contain the same object.

In our method, all instances of the same images are mapped to the same target point. Specifically, let  $g$  denote a random image transformation. Given a mini-batch of images  $X_b$ , we apply  $g$  to  $X_b$   $r$  times, effectively creating a batch of  $r \cdot b$  images. When computing point assignment, all  $r$  images are mapped to the same target point.

Why is this algorithmic ingredient useful? When training the convnet, it must find common patterns between the transformed images when fitting them to the same target. These common patterns are likely to appear in other images in the dataset belonging to the same class. This pushes the network to map images that contain the same objects closer to each other, in a similar manner to the beneficial effect of self-supervision.

### 3.4. Auxiliary task

While optimizing the clustering objective (1), the convnet model simultaneously learns image representation and partitions the images. The success of unsupervised clustering is highly correlated with the quality of the learnt representation. It has been repeatedly shown that self-supervision methods can significantly improve the quality of representations in an unsupervised learning scenario. To benefit from this idea, we employ RotNet [15],

	MNIST		Fashion		CIFAR-10		CIFAR-100		STL-10	
	NMI	ACC	NMI	ACC	NMI	ACC	NMI	ACC	NMI	ACC
k-means	0.499	0.572	0.511	0.471	0.087	0.228	0.083	0.129	0.124	0.192
AE+k-means	0.725	0.812	0.526	0.535	0.239	0.313	0.100	0.164	0.249	0.303
Spectral clustering [42]	0.663	0.696	0.630	0.551	0.103	0.247	0.090	0.136	0.098	0.159
DEC [40]	0.772	0.843	0.546	0.518	0.257	0.301	0.136	0.185	0.276	0.359
JULE [41]	0.913	0.964	0.608	0.563	0.192	0.272	0.103	0.137	0.182	0.277
DAC [5]	0.935	0.978	0.632	0.615	0.396	0.522	0.185	0.238	0.249	0.303
ADC [18]	-	0.987	-	-	-	0.293	-	0.160	-	0.478
ClusterGAN [13]	0.921	0.964	-	-	0.323	0.412	-	-	0.335	0.423
N2D [30]	0.942	0.979	<b>0.684</b>	0.672	-	-	-	-	-	-
IIC [22]	-	<b>0.992</b>	-	-	-	0.617	-	0.257	-	0.499 <sup>1</sup>
VGG (avg.)	0.963	0.981	0.601	0.656	0.422	0.534	0.189	0.243	0.471	0.576
VGG ( $\pm$ ste)	$\pm 0.007$	$\pm 0.007$	$\pm 0.016$	$\pm 0.021$	$\pm 0.010$	$\pm 0.021$	$\pm 0.002$	$\pm 0.003$	$\pm 0.007$	$\pm 0.010$
VGG (lowest loss)	<b>0.974</b>	0.991	0.648	0.711	0.460	0.606	0.190	0.243	0.485	0.599
VGG (majority)	0.972	0.990	0.647	<b>0.721</b>	0.465	0.599	0.178	0.235	<b>0.498</b>	<b>0.611</b>
ResNet (avg.)	-	-	-	-	0.550	0.670	0.252	0.287	0.428	0.519
ResNet ( $\pm$ ste)	-	-	-	-	$\pm 0.008$	$\pm 0.011$	$\pm 0.002$	$\pm 0.004$	$\pm 0.004$	$\pm 0.011$
ResNet (lowest loss)	-	-	-	-	<b>0.572</b>	<b>0.700</b>	<b>0.259</b>	<b>0.312</b>	0.443	0.525
ResNet (majority)	-	-	-	-	0.562	0.690	0.258	0.300	0.402	0.516

Table 1. **Unsupervised clustering results.** The results of our method are shown below the separation line, based on one of two convnet architectures - VGG or ResNet (see Section 4.1). In each case, we show the average result over multiple runs and standard error (ste). We also show ensemble-based results based on two selection criteria - lowest loss and majority vote (see Section 4.2). Above the separation line we list state of the art results for comparison, see review in Section 2. Unreported results are marked with (-).

which is a self-supervised learning algorithm that learns image features by training a convnet to predict image rotations. Specifically, images are rotated by  $r$  degrees ( $r \in \{0^\circ, 90^\circ, 180^\circ, 270^\circ\}$ ), and the model is subsequently trained to predict their rotation by optimizing the cross-entropy loss. RotNet produces competitive performance in representation learning benchmarks, and has been shown to benefit training in other tasks, when incorporated into a model as an auxiliary task [7, 14, 28]. We incorporate RotNet into our method, modifying the convnet training procedure to alternate between optimizing the main clustering task and this secondary auxiliary task.

### 3.5. Refinement Stage

As we have no prior knowledge regarding the size of the clusters, we begin by assuming that clusters’ sizes are equal. When this assumption cannot be justified, we propose to augment the algorithm with an additional step, performed after the main training is concluded. In this step the assumption is relaxed, while target points are iteratively reassigned based on the outcome of k-means applied to  $f_\theta(x_1), \dots, f_\theta(x_n)$ , and assigning image  $x_i$  to target  $\mu_j$  with label  $j \in [K]$  derived from the outcome of k-means. This method is similar to DeepCluster [4], proposed by Caron et al. as an approach for representation learning, where they perform the clustering on the latent vectors of the model and not the final output layer. A possible alternative method may start with this stage and discard the first one altogether, as this approach makes no assumption on the size of the

clusters. However, we found that starting off with reassigning labels based on k-means is not competitive and produces less accurate clusters, for example, training on MNIST results in an accuracy of 81% ( $\pm 2.67$ ).

## 4. Experiments

We tested our method on several image datasets that are commonly used as benchmark for clustering, see results in Table 1. For comparison, state of the art results are also shown in Table 1. In almost all cases our method improves on previous results significantly, with the exception of MNIST where our results match the state of the art<sup>1</sup>. Examples of clustering results on the STL-10 dataset of natural images are shown in Figure 3. The confusion matrix when clustering the challenging CIFAR-10 dataset is shown in Figure 4.

In the rest of this section we specify the implementation details of our method, and analyze the results. We describe two methods for model selection that improve the results when obtaining several clustering instances of a dataset. Finally, we report the results of an ablation study evaluating the various ingredients of the algorithm, which demonstrate how they contribute to its success.

<sup>1</sup>Note that with STL-10, IIC reports an accuracy of 0.596 when using the much larger unlabeled data segment that includes distractor classes.

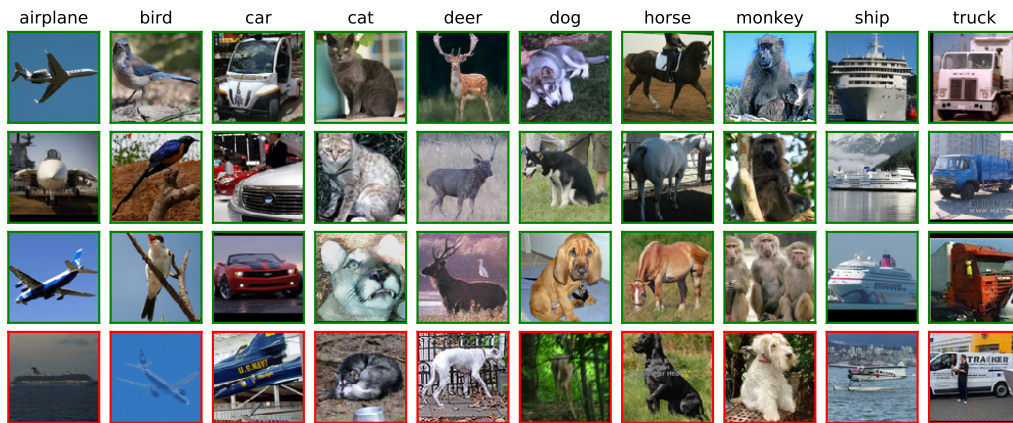


Figure 3. Unsupervised image clustering results on STL-10. Each column shows images from a different cluster. The top three images in each column are examples of images from the same class successfully clustered together. The images in the fourth row illustrate failure cases, where the image is assigned to the wrong cluster (e.g., an airplane assigned to the 'bird' cluster).

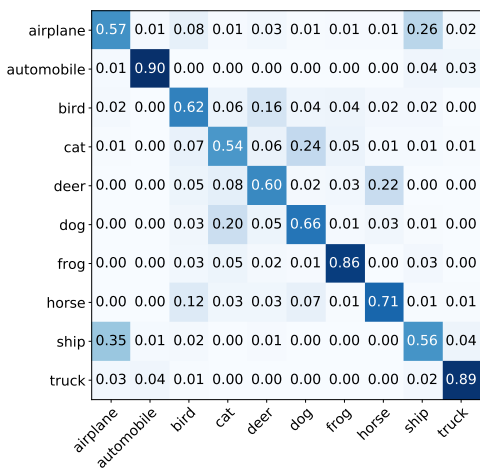


Figure 4. Results of unsupervised clustering by our method, showing the confusion matrix for CIFAR-10. Some classes are easier to separate from the others, such as automobiles, trucks and frogs. Most significant confusions are between ships and airplanes, cats and dogs, and deer and horses.

#### 4.1. Implementation details and evaluation scores

**Datasets.** Five different datasets are used in our empirical study. MNIST [27], Fashion-MNIST [39], CIFAR-10 [25], the 20 superclasses of CIFAR-100 [25], and STL-10 [8], see Table 2. We are most interested in the last 3 datasets because they consist of natural images. These datasets are commonly used to evaluate clustering methods.

Name	Classes	Samples	Dimension
MNIST	10	70,000	$28 \times 28$
Fashion-MNIST	10	70,000	$28 \times 28$
CIFAR-10	10	60,000	$32 \times 32 \times 3$
CIFAR-100	20	60,000	$32 \times 32 \times 3$
STL-10	10	13,000	$96 \times 96 \times 3$

Table 2. The image datasets used in our experiments.

**Architectures.** We describe experiments with two convnet architectures. The first is a VGG model [36] with batch normalization [20]. Each block in this neural network consists of two convolutions, each followed by a batch normalization layer and ReLU activation function, and ends with a max pooling layer. Our model has three blocks, except for STL-10, where we use four because images are larger. The second architecture is a ResNet model [19] with 34 layers. These base models are followed by a linear prediction layer, that outputs the cluster assignments. When trained on the auxiliary task, the base model is also followed by another head, consisting of three fully connected layers (multilayer perceptron), which predicts the image rotation.

**Training details.** The network is trained with stochastic gradient descent, momentum of 0.9 and  $\ell_2$  loss over the weights  $\theta$ . A learning rate of 0.05 is used for the VGG models and 0.01 for the ResNets. We use batch size of 128 and perform random image augmentations which include cropping, flipping and color jitter. When training on the clustering task, each mini-batch is augmented by  $r = 3$  random transformations, where all 3 repetitions that represent

the same image are mapped to the same target point. When training on the auxiliary rotation task, we rotate each image by all four orientations, resulting in an effective batch size of 512. As is commonly done in unsupervised learning algorithms [3, 4, 22], in order to avoid clustering based on trivial cues such as color, the images are pre-processed using Sobel filters.

**Mixture of Gaussians.** We examined several initialization heuristics to determine the Gaussian means  $\{\mu_k\}$  in the GMM distribution defined in (2), and concluded that using  $K$  different one-hot vectors in  $\mathbb{R}^K$  is most effective. A comparison of different initialization schemes is provided in Table 3. We set  $\Sigma_k = 0.05 \cdot I_{K \times K} \forall k \in [K]$ .

	accuracy	nmi
one-hot ( $d = 10$ )	97.47 ( $\pm 0.11$ )	94.16 ( $\pm 0.19$ )
uniform ( $d = 10$ )	96.6 ( $\pm 0.44$ )	92.68 ( $\pm 0.66$ )
uniform ( $d = 128$ )	93.04 ( $\pm 1.59$ )	88.96 ( $\pm 1.12$ )

Table 3. Comparison of different initialization schemes for the mixture of Gaussians mean vectors when clustering MNIST. All vectors lie on the  $d$ -dimensional unit sphere. Initialization schemes 2 and 3 are sampled from a multi-variate uniform distribution within the range  $[-0.1, 0.1]$  and projected onto the unit sphere. Other than varying the mean vectors, the training procedure is the same, and does not include the refinement stage.

**Evaluation scores.** To evaluate clustering performance we adopt two commonly used scores: Normalized Mutual Information (NMI), and Clustering Accuracy (ACC). Clustering accuracy measures the accuracy of the hard-assignment to clusters, with respect to the best permutation of the datasets ground-truth labels. Normalized Mutual Information measures the mutual information between the ground-truth labels and the predicted labels based on the clustering method. The range of both scores is  $[0, 1]$ , where a larger value indicates more precise clustering results. We use center crops of images for evaluation.

## 4.2. Ensemble of networks

Different executions of the algorithm using the same dataset lead to non-negligible variations in clustering quality as evaluated by the two clustering scores - ACC and NMI. This happens due to the stochastic nature of the method, with the random initialization of parameters, mini-batch sampling and random image transformations. A clustering ensemble can be beneficial (cf. [6]), and we propose two methods to improve the clustering results based on an ensemble of networks. We report results with both methods in Table 1.

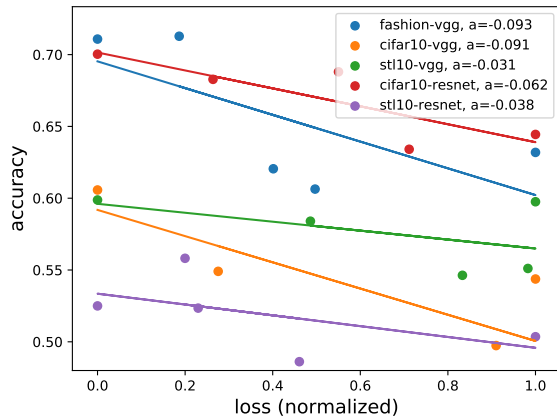


Figure 5. Clustering accuracy as a function of model loss.

**Lowest loss.** When comparing the train loss of the network with its clustering scores in multiple runs, we noticed a significant positive correlation between them as shown in Figure 5. A possible explanation for this empirical result is that if the mapping  $P : [n] \rightarrow [n]$  assigns an image to a bad target point, its neighbors are likely to be points from another class, and the convnet’s attempt to generalize will not produce a good fit for that point resulting in higher loss.

**Majority vote.** We implement majority voting as a strategy to combine the solutions of a clustering ensemble. Without ground-truth labels this task is not trivially solved, as the absolute clustering labels are arbitrary and do not necessarily align between multiple clustering solutions. To circumvent this, we fix one solution, specifically the one with the lowest loss. We then find for each other clustering solution the permutation that most agrees with the fixed one, using once again the Hungarian algorithm [26].

## 4.3. Analysis

The results of our method when applied to five image datasets are reported in Table 1. Clearly, our clustering algorithm is able to separate unlabeled images into distinct groups of semantically similar images with high accuracy, improving the state-of-the-art in four of the more challenging datasets. Using an ensemble of clustering networks almost always improves the results over the average.

Figure 4 shows the confusion matrix obtained by the algorithm when partitioning the very challenging CIFAR-10 dataset, without using its labels. The majority of images in each cluster correspond to one of the 10 object classes in a unique manner, where most of the false assignments correspond to images from semantically similarly looking objects such as cats and dogs, deer and horse, or airplanes

and ships. It is interesting that the smaller VGG architecture performs better on the STL-10 dataset as compared to ResNet, possibly because the more limited capacity of the smaller VGG model is able to generalize better on the smaller dataset.

The auxiliary task in our method, which is added to the clustering task, is based on image rotation and is designed for natural images. We use it to enhance the clustering of CIFAR-10, CIFAR-100 and STL-10. In order to verify that this auxiliary task is not the sole reason for the method’s success, we trained the model with the auxiliary task alone on CIFAR-10, and then clustered the images by applying k-means to the output of the last layer of the base model. This method achieved an accuracy of 0.385, much lower than the accuracy achieved by our algorithm.

#### 4.4. Ablation study

Next we describe the results of an ablation study examining the critical components of the algorithm. We start with the basic model based on VGG, without image repetitions, and without optimizing the auxiliary task. We then add image repetitions. Then we add the auxiliary task, training to predict rotation angle. Finally, we replace the simpler VGG architecture with the bigger and more effective ResNet architecture, which requires more resources to train. We use the CIFAR-10 dataset as our study case. Results are shown in Table 4, illustrating how each component contributes to the performance of the final algorithm. In Figure 6 we show how the training curves change with each added component.

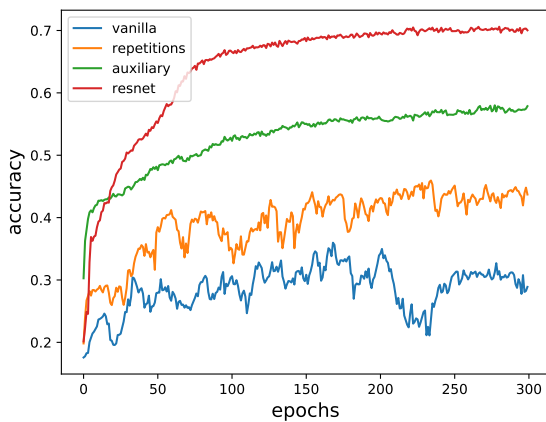


Figure 6. Training curves of different configurations in the ablation study. Adding the methods’ components improves model accuracy and stability. Note that the VGG based configurations are trained for more epochs than showed.

**Refinement stage.** We compare clustering performance with and without the proposed refinement stage in Table 5.

	CIFAR-10
Vanilla	0.28
Image repetitions	0.48
Auxiliary task	0.60
ResNet	0.70

Table 4. **Ablation study.** Each row corresponds to the addition of one component in our method. The last row corresponds to the full configuration.

MNIST is the only dataset with class imbalance, as its smallest class has 6313 samples while its largest has 7877. The refinement stage helps the algorithm achieve near perfect clustering with accuracy of 99.1%.

	Before	After
MNIST	0.971	0.991
Fashion	0.721	0.723
CIFAR-10	0.700	0.697
CIFAR-100	0.312	0.287
STL-10	0.611	0.606

Table 5. Comparison of clustering performance with and without the refinement stage.

## 5. Summary and discussion

We presented an end-to-end deep clustering method, which out-performs all other clustering methods when applied to unlabeled natural images. The variant of our method, which is based on running the algorithm repeatedly and choosing the solution that achieves the minimal train loss, leads to very significant improvement in the state of the art: for CIFAR-10 accuracy is improved from 62% to 70%, for CIFAR-100 accuracy is improved from 26% to 31%, and for STL-10 accuracy is improved from 50% to 52% when using ResNet and to 61% when using VGG.

The algorithm is relatively efficient, using off the shelf deep learning components such as ResNet or VGG. We note that our method is quite robust - the same hyper-parameters were used in all the experiments reported above. In order to deal with unbalanced datasets, we discussed a refinement stage which improved performance on the somewhat unbalanced MNIST dataset, without significantly affecting the results on the remaining 4 balanced datasets. Unbalanced datasets pose a challenge to all unsupervised clustering methods, a challenge which will be addressed in our future work.

The basic ingredient of our method is based on a recent unsupervised representation learning method [3], demonstrating once again how the problems of unsupervised representation learning and clustering are connected, and how progress in one can advance the other.



## References

- [1] David Arthur and Sergei Vassilvitskii. K-means++: The advantages of careful seeding. volume 8, pages 1027–1035, 01 2007. [2](#)
- [2] Y. Bengio, Pascal Lamblin, D. Popovici, Hugo Larochelle, and U. Montreal. Greedy layer-wise training of deep networks. volume 19, 01 2007. [2](#)
- [3] P. Bojanowski and A. Joulin. Unsupervised learning by predicting noise. In *ICML*, 2017. [1](#), [2](#), [3](#), [7](#), [8](#)
- [4] Mathilde Caron, Piotr Bojanowski, Armand Joulin, and Matthijs Douze. Deep clustering for unsupervised learning of visual features. In *European Conference on Computer Vision*, 2018. [2](#), [5](#), [7](#)
- [5] Jianlong Chang, Lingfeng Wang, Gaofeng Meng, Shiming Xiang, and Chunhong Pan. Deep adaptive image clustering. *2017 IEEE International Conference on Computer Vision (ICCV)*, pages 5880–5888, 2017. [2](#), [5](#)
- [6] Masoud Charkhabi, Tarundeep Dhot, and Shirin Mojarad. Cluster ensembles, majority vote, voter eligibility and privileged voters. *International Journal of Machine Learning and Computing*, 4:275–278, 06 2014. [7](#)
- [7] Ting Chen, Xiaohua Zhai, Marvin Ritter, Mario Lui, and Neil Houlsby. Self-supervised gans via auxiliary rotation loss. 2018. [2](#), [5](#)
- [8] Adam Coates, Andrew Ng, and Honglak Lee. An analysis of single-layer networks in unsupervised feature learning. *Journal of Machine Learning Research - Proceedings Track*, 15:215–223, 01 2011. [6](#)
- [9] Carl Doersch, Abhinav Gupta, and Alexei A. Efros. Unsupervised visual representation learning by context prediction. *2015 IEEE International Conference on Computer Vision (ICCV)*, pages 1422–1430, 2015. [2](#)
- [10] Carl Doersch and Andrew Zisserman. Multi-task self-supervised visual learning. In *Proceedings of the IEEE International Conference on Computer Vision*, pages 2051–2060, 2017. [2](#)
- [11] Richard O Duda and Peter E Hart. Pattern recognition and scene analysis, 1973. [2](#)
- [12] Carsten Gerlhof, Alfons Kemper, Christoph Kilger, and Guido Moerkotte. Partition-based clustering in object bases: From theory to practice. In *International Conference on Foundations of Data Organization and Algorithms*, pages 301–316. Springer, 1993. [2](#)
- [13] Kamran Ghasedi, Xiaoqian Wang, Cheng Deng, and Heng Huang. Balanced self-paced learning for generative adversarial clustering network. In *CVPR*, 2019. [5](#)
- [14] Spyros Gidaris, Andrei Bursuc, Nikos Komodakis, Patrick Pérez, and Matthieu Cord. Boosting few-shot visual learning with self-supervision. *ArXiv*, abs/1906.05186, 2019. [5](#)
- [15] Spyros Gidaris, Praveer Singh, and Nikos Komodakis. Unsupervised representation learning by predicting image rotations. In *International Conference on Learning Representations*, 2018. [2](#), [4](#)
- [16] Ian J. Goodfellow, Jean Pouget-Abadie, Mehdi Mirza, Bing Xu, David Warde-Farley, Sherjil Ozair, Aaron Courville, and Yoshua Bengio. Generative adversarial nets. In *Proceedings of the 27th International Conference on Neural Information Processing Systems - Volume 2, NIPS’14*, pages 2672–2680, Cambridge, MA, USA, 2014. MIT Press. [2](#)
- [17] K. Chidananda Gowda and G. Krishna. Agglomerative clustering using the concept of mutual nearest neighbourhood. *Pattern Recognition*, 10:105–112, 1978. [2](#)
- [18] Philip Häusser, Johannes Plapp, Vladimir Golkov, Elie Aljalbout, and Daniel Cremers. Associative deep clustering: Training a classification network with no labels. In *GCPR*, 2017. [2](#), [5](#)
- [19] Kaiming He, Xiangyu Zhang, Shaoqing Ren, and Jian Sun. Deep residual learning for image recognition. In *Proceedings of the IEEE conference on computer vision and pattern recognition*, pages 770–778, 2016. [6](#)
- [20] Sergey Ioffe and Christian Szegedy. Batch normalization: Accelerating deep network training by reducing internal covariate shift. *ArXiv*, abs/1502.03167, 2015. [6](#)
- [21] Anil K Jain, M Narasimha Murty, and Patrick J Flynn. Data clustering: a review. *ACM computing surveys (CSUR)*, 31(3):264–323, 1999. [1](#)
- [22] Xu Ji, João F Henriques, and Andrea Vedaldi. Invariant information clustering for unsupervised image classification and segmentation. In *Proceedings of the IEEE International Conference on Computer Vision*, pages 9865–9874, 2019. [3](#), [5](#), [7](#)
- [23] Diederik Kingma and Max Welling. Auto-encoding variational bayes. 12 2014. [2](#)
- [24] Hans-Peter Kriegel, Peer Kröger, Jörg Sander, and Arthur Zimek. Density-based clustering. *Wiley Interdisciplinary Reviews: Data Mining and Knowledge Discovery*, 1(3):231–240, 2011. [2](#)
- [25] Alex Krizhevsky. Learning multiple layers of features from tiny images. *University of Toronto*, 05 2012. [6](#)
- [26] H. W. Kuhn and Bryn Yaw. The hungarian method for the assignment problem. *Naval Res. Logist. Quart.*, pages 83–97, 1955. [3](#), [7](#)
- [27] Yann Lecun, Lon Bottou, Yoshua Bengio, and Patrick Haffner. Gradient-based learning applied to document recognition. In *Proceedings of the IEEE*, pages 2278–2324, 1998. [6](#)
- [28] Mario Lui, Marvin Ritter, Michael Tschannen, Xiaohua Zhai, Olivier Frederic Bachem, and Sylvain Gelly. High-fidelity image generation with fewer labels. In *International Conference on Machine Learning*, 2019. [5](#)
- [29] Jonathan Masci, Ueli Meier, Dan C. Ciresan, and Jürgen Schmidhuber. Stacked convolutional auto-encoders for hierarchical feature extraction. In *ICANN*, 2011. [2](#)
- [30] Ryan McConville, Raúl Santos-Rodríguez, Robert J. Piechocki, and Ian Craddock. N2d: (not too) deep clustering via clustering the local manifold of an autoencoded embedding. *ArXiv*, abs/1908.05968, 2019. [5](#)
- [31] Erxue Min, Xifeng Guo, Qiang Liu, Gen Zhang, Jianjing Cui, and Jun Long. A survey of clustering with deep learning: From the perspective of network architecture. *IEEE Access*, 6:39501–39514, 2018. [1](#)
- [32] Mehdi Noroozi and Paolo Favaro. Unsupervised learning of visual representations by solving jigsaw puzzles. *ArXiv*, abs/1603.09246, 2016. [2](#)

- [33] R. Ostrovsky, Y. Rabani, L. J. Schulman, and C. Swamy. The effectiveness of lloyd-type methods for the k-means problem. In *2006 47th Annual IEEE Symposium on Foundations of Computer Science (FOCS'06)*, pages 165–176, Oct 2006. [2](#)
- [34] Deepak Pathak, Philipp Krahenbuhl, Jeff Donahue, Trevor Darrell, and Alexei Efros. Context encoders: Feature learning by inpainting. 04 2016. [2](#)
- [35] Maurice Roux. A comparative study of divisive hierarchical clustering algorithms, 2015. [2](#)
- [36] Karen Simonyan and Andrew Zisserman. Very deep convolutional networks for large-scale image recognition. *arXiv 1409.1556*, 09 2014. [6](#)
- [37] Pascal Vincent, Hugo Larochelle, Isabelle Lajoie, Yoshua Bengio, and Pierre-Antoine Manzagol. Stacked denoising autoencoders: Learning useful representations in a deep network with a local denoising criterion. *J. Mach. Learn. Res.*, 11:3371–3408, Dec. 2010. [2](#)
- [38] W. Wang, Y. Wu, C. Tang, and M. Hor. Adaptive density-based spatial clustering of applications with noise (dbscan) according to data. In *2015 International Conference on Machine Learning and Cybernetics (ICMLC)*, volume 1, pages 445–451, July 2015. [2](#)
- [39] Han Xiao, Kashif Rasul, and Roland Vollgraf. Fashion-mnist: a novel image dataset for benchmarking machine learning algorithms, 2017. [6](#)
- [40] Junyuan Xie, Ross B. Girshick, and Ali Farhadi. Unsupervised deep embedding for clustering analysis. In *ICML*, 2015. [5](#)
- [41] Jianwei Yang, Devi Parikh, and Dhruv Batra. Joint unsupervised learning of deep representations and image clusters. In *IEEE Conference on Computer Vision and Pattern Recognition (CVPR)*, 2016. [2](#), [5](#)
- [42] Lih Zelnik-Manor and Pietro Perona. Self-tuning spectral clustering. In *Proceedings of the 17th International Conference on Neural Information Processing Systems, NIPS'04*, pages 1601–1608, Cambridge, MA, USA, 2004. MIT Press. [5](#)
- [43] Junbo Zhao, Michael Mathieu, Ross Goroshin, and Yann Lecun. Stacked what-where auto-encoders. 06 2015. [2](#)